北京航空航天大学四年级博士生和五年级直博生
学校奖学金申报表

（请按填表说明填写，本表填写的内容必须为非涉密可公开!）

<table>
<tr><td>姓　名</td><td>王蕊</td><td>学　号</td><td>BY1510119</td><td>指导教师</td><td colspan="2">李晓明，牛海军</td></tr>
<tr><td>类　别</td><td colspan="3">✔ 三年级博士生　☐ 四年级直博生</td><td>学科/专业</td><td colspan="2">生物医学工程</td></tr>
<tr><td rowspan="4">承担科研任务情况</td><td colspan="2">项目名称</td><td>课题来源</td><td>课题负责人</td><td colspan="2">本人承担的具体工作</td></tr>
<tr><td colspan="2">基于超声共振谱技术的模拟失重尾吊大鼠皮质骨的细观力学特性研究</td><td>06</td><td>牛海军</td><td colspan="2">小尺寸非规则体生物硬组织材料的弹性性质的超声共振谱测量技术研究</td></tr>
<tr><td colspan="2"></td><td></td><td></td><td colspan="2"></td></tr>
<tr><td colspan="7"></td></tr>
<tr><td rowspan="14">已取得研究成果（论文、专利、获奖等）</td><td>论文题目</td><td>本人排名</td><td>发表年月</td><td>期刊（会议）名称</td><td colspan="2">被检索类型</td></tr>
<tr><td>The Elasticity Coefficients Measurement of Human Dentin Based on RUS</td><td>3</td><td>2017.4</td><td>BioMed Research International</td><td colspan="2">1</td></tr>
<tr><td>Measurement of Human Enamel Mechanical Characteristics with Resonant Ultrasound Spectroscopy</td><td>3</td><td>2017.7</td><td>The 39th Annual International Conference of the IEEE Engineering in Medicine and Biology Society</td><td colspan="2">(Poster)</td></tr>
<tr><td>基于超声共振谱方法的人牙釉质材料力学特性研究</td><td>3</td><td>2017.10</td><td>医用生物力学</td><td colspan="2">11</td></tr>
<tr><td></td><td></td><td></td><td></td><td colspan="2"></td></tr>
<tr><td>专利名称</td><td>本人排名</td><td>发布年月</td><td>专利号</td><td colspan="2">专利类型</td></tr>
<tr><td></td><td></td><td></td><td></td><td colspan="2"></td></tr>
<tr><td></td><td></td><td></td><td></td><td colspan="2"></td></tr>
<tr><td>获科技成果奖励名称</td><td>本人排名</td><td>获奖年月</td><td>证书编号</td><td colspan="2">奖励级别</td></tr>
<tr><td></td><td></td><td></td><td></td><td colspan="2"></td></tr>
<tr><td></td><td></td><td></td><td></td><td colspan="2"></td></tr>
<tr><td>本人承诺</td><td colspan="6">本人所填写的以上内容均为真实情况。
本人签字：_____
年　月　日</td></tr>
</table>

导师 意见	同意 / 不同意 该同学申报学校奖学金。 导师签字：_____ 年 月 日
学院学位 评定分委 员会意见	同意 / 不同意 该同学获得学校奖学金。 签字：_____ （学院代盖） 年 月 日

Measurement of Human Enamel Mechanical Characteristics with Resonant Ultrasound Spectroscopy

FENG Dandan, FAN Fan, WANG Rui, ZHANG Qiang, NIU Haijun*

Abstract— **The measurement of enamel mechanical properties offers great significance for the design, development and evaluation of clinical dental restorative materials. In this paper, resonant ultrasound spectroscopy (RUS) was proposed to measure the full second-order elastic tensor of human enamel specimens, and the mechanical parameters of human enamel, including Young's moduli, shear moduli and Poisson's ratios, were further calculated, which ranged from 64.50 to 80.46 GPa, 26.63 to 51.86 GPa and 0.18 to 0.40, separately. This study demonstrates that RUS shows feasibility on measuring the mechanical properties of human enamel with repeatable and nondestructive advantages.**

I. Introduction

Human teeth are mainly composed of enamel, dentin and dental pulp. Enamel covers the crown surface and protects the inner tissues. As the hardest tissue of human tooth, enamel contains inorganic (mainly hydroxyapatite, 96% ~ 97% in mass), organic and water [1]. Moreover, enamel is nonrenewable once abraded or eroded so that alternative materials are needed for repairing or rebuilding [2]. The structure and function of enamel are closely related to its mechanical properties.

The methods of measuring enamel mechanical properties mainly include stretching, compression, acoustic method in macro scale and nano-indentation in micro scale. These methods promote the understanding of macro and micro mechanical properties of enamel, which have a vital significance for the development, design, preparation and clinical evaluation of dental restorative materials. However, these methods have their certain drawbacks. For example, stretching and compression methods are destructive, and require a larger volume of specimen, which is difficult to acquire for human enamel. Despite of the nondestructive feature, acoustic method has the same requirement to volume limited by the ultrasound wavelength. Nano-indentation is good at calculating the elastic moduli in different directions of small-sized specimen. However, the results mainly reflect the mechanical properties of microstructure, which are different in macro scale. All along, the measurement results of enamel mechanical properties vary widely. Ye De Lin *et al* [3] measured the elastic modulus of human molar enamel at the range of 24.9 to 26.8 GPa by stretching method. Craig *et al* [4] compressed human enamel specimen, and determined its elastic modulus (62.74 ~ 95.84 GPa). Cuy JL MA *et al* [5] measured the elastic modulus of human enamel by nano-indentation method, which was greater than 115 GPa.

Resonant ultrasound spectroscopy (RUS) has been developed as an accurate and efficient method to characterize the material mechanical properties [6]. In recent years, Pascal *et al* have applied RUS to bone materials, which broke the limit of RUS for measuring elastic constants of low Q (quality factor) materials [7]. All elastic constants of an extremely small specimen (even less than 1 mm) can be measured in one nondestructive experiment with high reproducibility.

The purpose of this paper was to investigate the mechanical properties of enamel based on RUS. The elastic constants of human enamel were extracted, and the mechanical parameters, such as Young's moduli, shear moduli and Poisson's ratios, were calculated and compared with previous researches.

II. Experiments and Method

Three steps of RUS are shown in Fig.1. The theoretical resonant frequencies are calculated with specimen's mass, dimensions and the initial elastic constants from the prior knowledge. Then, the experimental resonant frequencies was measured and extracted from RUS experiments. Finally, an iterative procedure is used to adjust the elastic constants of enamel until the theoretical frequencies correspond to the experimental frequencies based on minimum mean-squared error criterion, then the mechanical parameters including Young's moduli, shear moduli and Poisson's ratios were calculated based on the optimal elastic constants.

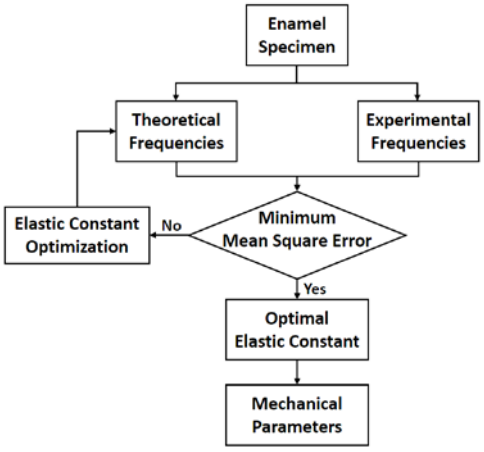

Fig.1 The flow chart of RUS.

*Research supported by the National Natural Science Foundation of China (31570945) and the National Science and Technology Support Program (2015BAI06B02).

FENG Dandan, FAN Fan, WANG Rui, ZHANG Qiang and NIU Haijun are with the Key Laboratory of Ministry of Education for Biomechanics and Mechanobiology, School of Biological Science and Medical Engineering, Beihang University, Beijing, China (*corresponding author: phone: +86-010-82339152; fax: +86-010-82339152; e-mail: hjniu@buaa.edu.cn).

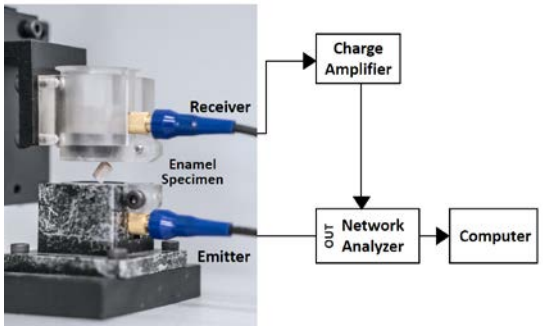

Fig.2 The block diagram of the experimental setup.

A. Experimental system

Fig.2 shows the schematic of experimental system. The enamel specimen was mounted on opposing corners between two shear wave transducers (V154RM, Panametrics Inc. Waltham, US). Firstly, a network analyzer (Bode 100, Omicron electronics GmbH, Klaus, Austria) was used to output a swept-frequency signal as the excitation of the emitter. The resonant signals were amplified by a broadband amplifier (HQA-15M-10T, Femto Messtechnik GmbH, Berlin, Germany), recorded by the vector network analyzer, imported to the computer and processed.

B. Specimen preparations

The specimens used in this study, collected from the Peking University Hospital of stomatology, were three healthy molars from three 27-year-old young women, respectively. Firstly, the tartars and granulations from the tooth surface were removed. Then, a slow speed diamond saw (SYJ-150, precision 0.01mm) was used to cut the enamel roughly. After polished by 500-mesh, 800-mesh and 2000-mesh abrasive papers, the standard rectangular parallelepiped specimen was made. The specimens were stored in saline in hydrated state. Dimensions were measured using a digital caliper (accuracy: ±0.02 mm) and shown in TABLE 1.

TABLE 1 THE BASIC INFORMATION OF ENAMEL SPECIMENS

Specimen	Length /mm	Width /mm	Thickness /mm	Mass/ mg
1	3.683	3.040	1.660	51
2	3.070	1.980	1.867	31
3	3.240	2.120	1.647	30

C. Resonant frequency measurement

In the RUS experiment, the enamel specimens were placed between two transducers, as shown in Fig.2. The frequency response of the specimen was measured within 0.32 and 1.35 MHz with 100 Hz resolution. Six independent experiments were performed on each enamel specimen with same parameters and six groups of experimental resonant frequencies were obtained by seeking local maximum points. We selected the frequencies presented at least three times out of six, and calculated their mean values, standard deviations (SD) and coefficient variations (coefficient variation = standard deviation/mean*100%, CV). The mean values of selected frequencies with standard deviations less than 2 kHz and the coefficient variations under 0.3% were considered the experimental resonant frequencies.

D. Theoretical resonant frequency calculation

According to the results of the finite element analysis [8], human enamel is assumed to be a transversely isotropic and inviscid material, with five independent constants. The initial values of elastic coefficients were adopted from the above paper [8]: C_{11} = 82.96 GPa, C_{12} = 36.04 GPa, C_{13} = 34.66 GPa, C_{33} = 92.89 GPa, C_{44} = 22.90 GPa.

$$C_{ij} = \begin{pmatrix} C_{11} & C_{12} & C_{13} & 0 & 0 & 0 \\ C_{12} & C_{11} & C_{13} & 0 & 0 & 0 \\ C_{13} & C_{13} & C_{33} & 0 & 0 & 0 \\ 0 & 0 & 0 & C_{44} & 0 & 0 \\ 0 & 0 & 0 & 0 & C_{44} & 0 \\ 0 & 0 & 0 & 0 & 0 & \frac{1}{2}(C_{11}-C_{12}) \end{pmatrix} \quad (1)$$

Based on the Einstein's summation convention, given the constants in C_{ij}, the theoretical resonant frequencies of enamel specimen can be obtained by finding the stationary points of the Lagrangian L:

$$L = \frac{1}{2}\int \left[(\rho(2\pi f)^2 u_i{}^2 - C_{ijkl}\frac{\partial u_i}{\partial x_j}\frac{\partial u_k}{\partial x_l}) \right] dV \quad (2)$$

With ρ and V respectively the specimen's density and volume, C_{ijkl} the initial elastic constants, f the resonant frequencies and u_i the displacement fields. The equation was solved by Rayleigh-Ritz method. The specific procedure was described in [9] and not repeated here.

E. Mechanical constants extractions

After obtaining the experimental and theoretical resonant frequencies of the enamel specimen, the cost function $F(C)$ can be defined as

$$F(C) = \sum_{i=1}^{N} w_i (f_i^{exp} - f_i^{cal}(C))^2 \quad (3)$$

Where N is the number of experimental resonant frequencies, C is the elastic constants of enamel, f_i^{cal} is the i -th theoretical resonant frequency, f_i^{exp} is the i -th experimental resonant frequency and w_i is the weight, which is shown in (4):

$$w_i = \begin{cases} 0 & f_i^{cal}\ does\ not\ match\ f_i^{exp} \\ 1/(f_i^{exp})^2 & f_i^{cal}\ matches\ f_i^{exp} \end{cases} \quad (4)$$

Levenberg-Marquardt (LM) method was applied to minimize the value of $F(C)$ by adjusting the elastic constants [10]. Under the convergent condition, the optimal elastic constants C was the ones that minimized $F(C)$. According to the generalized Hooke's law, the mechanical parameters can be further calculated.

III. RESULTS

The experimental spectrums of an enamel specimen are shown in Fig.3. We selected 18 resonance peaks as the experimental resonant frequencies based on the criterion mentioned above.

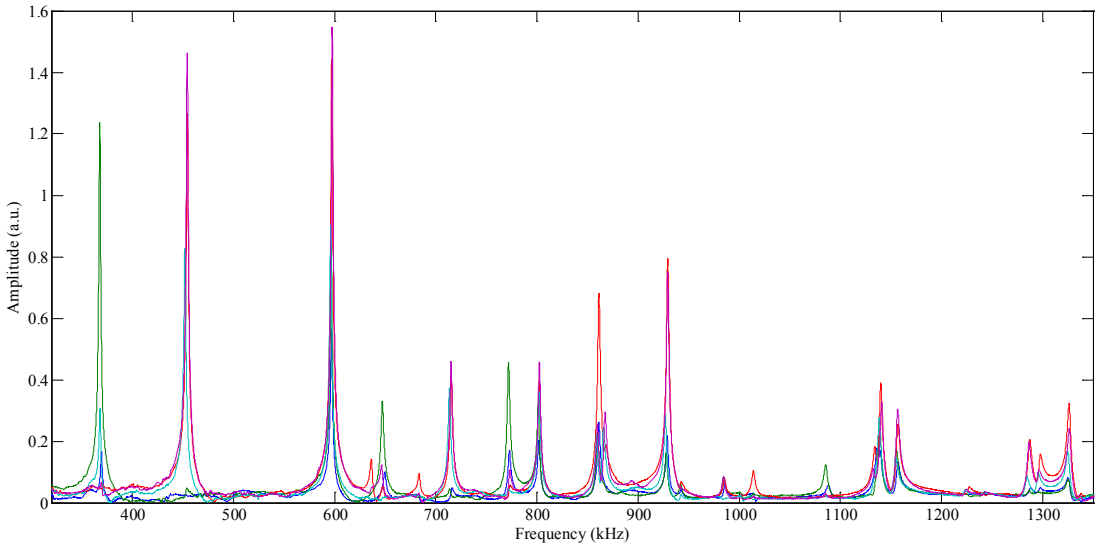

Fig.3 Experimental spectrums of an enamel specimen.

TABLE 2 THE ELASTIC CONSTANTS OF THE ENAMEL SPECIMENS

Specimen	C_{11} /GPa	C_{12} /GPa	C_{13} /GPa	C_{33} /GPa	C_{44} /GPa
1	92.04	26.30	32.68	94.13	29.65
2	96.72	43.46	23.41	72.32	51.86
3	96.63	30.53	31.89	83.57	32.61

TABLE 3 THE MECHANICAL PARAMETERS OF THE ENAMEL SPECIMENS

Specimen	E_{11} /GPa	E_{33} /GPa	ν_{12}	ν_{13}	G_{13} /GPa	G_{12} /GPa
1	77.92	76.08	0.18	0.28	29.65	32.87
2	74.69	64.50	0.40	0.19	51.86	26.63
3	80.46	67.57	0.22	0.30	32.61	33.05

The elastic constants of the three enamel specimens are shown in TABLE 2, where C_{11} is in the range of 92.04 ~ 96.72 GPa, C_{12} is 26.30 ~ 43.46 GPa, C_{13} is 23.41 ~ 32.68 GPa, C_{33} is 72.32 ~ 94.13 GPa and C_{44} is 29.65 ~ 51.86 GPa, respectively.

TABLE 3 shows the mechanical parameters of the three enamel specimens. Young's moduli, E_{11} and E_{33} are from 74.69 to 80.46GPa and from 64.50 to 76.08GPa, respectively. Poisson's ratio, ν_{12} and ν_{13} are between 0.18 ~ 0.40 and 0.19 ~ 0.30, respectively. Shear moduli, G_{13} and G_{12} are from 29.65 to 51.86 GPa and from 26.63 to 32.87 GPa, respectively.

IV. DISCUSSION

The elastic properties of human tooth are of paramount importance in all discussions of tooth strength, including Young's modulus, shear modulus and Poisson's ratio. In this paper, RUS was applied to measure the elastic constants and calculate mechanical parameters of human enamel.

As a relatively stiff biomaterial, the resonant peaks of enamel are sharp and experimental resonant frequencies could be extracted with no ambiguity. With considerate experimental operation, the errors are mainly from theoretical model and frequency-fitting. According to the scant researches on enamel symmetry [8], enamel were assumed to be transversely isotropic material with five independent constants in this paper, which may be not adequate for the real situation. The assumption of higher symmetry should be introduced in our future study to acquire more accurate constant properties of human enamel. We adopted the so-called trial and error method [11], combined with manual intervention to do the frequency-fitting, and LM method for the mechanical constants optimization. And a final elastic tensor that minimized the cost function was obtained with carefully choice of the initial elastic constants values. However, the accuracy and robustness of the fitting and optimization steps remained to be further verified.

In the past decades, the range of enamel's Young's modulus was large. Early, Ye De Lin *et al* found human molar enamel modulus between 24.9 and 26.8 GPa using stretching method [3], and Poisson ratio from 0.15 to 0.36 [12]. Stanford *et al* measured the Young's modulus of the tip enamel to be 56.5 GPa [13]. Craig *et al* compressed human enamel specimen, and determined its Young's modulus range of 62.74 to 95.84 GPa [4]. In this paper, Young's modulus of the enamel measured by RUS is from 64.5 ~ 80.46 GPa, consistent with the result of Craig and larger than others'; Poisson's ratio is between 0.18 and 0.40, which was in agreement with the results of Ye De Lin.

The reason why Ye De Lin and Stanford measured smaller Young's modulus may be the difficulty in making enamel specimen. Some dentin or small defects could be contained in enamel specimen. Craig *et al* have pointed out the low value of previous results may be due to the interference of the specimen itself [4]. In addition, the measurement error caused by clamping the small-sized specimen in traditional mechanical tests, such as stretching or compression, may also affect the results.

V. Conclusion

In conclusion, the results of this study preliminary demonstrated the feasibility of RUS in measuring mechanical properties of human enamel and its non-destructive measurement advantages. In the next work, the number of enamel specimens would be enlarged to further confirm the effectiveness of this method and explain the mechanical properties of enamel more comprehensively. This paper could provide valuable information for the dental material development and oral mechanics research.

References

[1] H. H. Li, M. V. Swain, "Understanding the mechanical behavior of human enamel from its structural and compositional characteristics," *Journal of the Mechanical Behavior of Biomedical Materials*, vol.1, no.1, pp. 18-29, 2008.

[2] K. Chun, H. Choi, J. Lee, "Comparison of mechanical property and role between enamel and dentin in the human teeth," *Journal of Dental Biomechanics*, vol.5, no.1, pp. 1758736014520809, 2014.

[3] D. L. Ye, "Measurement of modulus of human enamel with resistance strain measurement technique," *West China Journal of Stomatology*, no.3, pp. 207-209, 1991.

[4] R. G. Craig, F. A. Peyton, D. W. Johnson, "Compressive properties of enamel, dental cements, and gold," *Journal of Dental Research*, vol.40, no.5, 1961.

[5] J. L. Cuy, A. B. Mann, K. J. Livi, "Nanoindentation mapping of the mechanical properties of human molar tooth enamel," *Archives of Oral Biology*, vol.47, no.4, pp. 281-291, 2002.

[6] A. Migliori, J. D. Maynard, "Implementation of a modern resonant ultrasound spectroscopy system for the measurement of the elastic moduli of small solid specimens," *Review of Scientific Instruments*, vol. 76, no. 12, pp. 121301-7, 1993.

[7] S. Bernard, Q. Grimal, P. Laugier, "Accurate measurement of cortical bone elasticity tensor with resonant ultrasound spectroscopy," *Journal of the Mechanical Behavior of Biomedical Materials*, vol. 18, no. 18C, pp. 12-19, 2013.

[8] M. Wen, J. Zheng, Z. R. Zhou, "Finite element analysis on effect of organic phase on mechanical properties of human tooth enamel," *Lubrication Engineering*, vol. 39, no. 7, pp. 21-25, 2014.

[9] A. Migliori, JL. Sarrao, *Resonant ultrasound spectroscopy: applications to physics, materials measurements, and nondestructive evaluation*, Wiley, New York, 1997.

[10] S. Bernard, Q. Grimal, P. Laugier, "Resonant ultrasound spectroscopy for viscoelastic characterization of anisotropic attenuative solid materials," *Journal of the Acoustical Society of America*, vol. 135, no. 5, pp. 2601-13, 2014.

[11] M. Landa, P. Sedlák, H. Seiner, "Modal resonant ultrasound spectroscopy for ferroelastics," *Applied Physics A,* vol. 96, no. 3, pp. 557-567, 2009.

[12] D. L. Ye, Y. R. Su, B. Wang, "Measurement of Poisson's ratio of human enamel," *West China Journal of Stomatology*, no. 4, pp. 295–297, 1994.

[13] J. W. Stanford, G. C. Paffenbarger, J. W. Kumpula, "Determination of some compressive properties of human enamel and dentin," *Journal of the American Dental Association*, vol. 57, no. 4, pp. 487-495, 1958.

文章编号: 1004-7220(2017)05-0448-06

基于超声共振谱方法的人牙釉质材料力学特性研究

冯丹丹, 樊 璠, 王 蕊, 张 强, 牛海军
(北京航空航天大学 生物与医学工程学院, 北京 100191)

摘要: 目的 基于超声共振谱(resonant ultrasound spectroscopy, RUS)方法研究人牙釉质材料的力学特性。**方法** 制作长方体状牙釉质样本。估计样本的理论共振频率,与RUS实验测量得到的样本实际共振频率相比较。基于迭代方法调整牙釉质弹性常数,使得理论共振频率和实验共振频率满足均方误差最小准则,并计算弹性模量、剪切模量与泊松比。**结果** 牙釉质样本的弹性模量、剪切模量和泊松比范围分别为61.52~80.46 GPa、21.51~51.86 GPa和0.18~0.43。如果排除差异较大样本的影响,牙釉质的平均弹性模量、剪切模量和泊松比分别为72.84 GPa、31.94 GPa和0.27。**结论** RUS方法在测量牙釉质力学特性方面具有可行性与重复性无损测量优势,一次测量就可以实现牙釉质所有弹性常数和力学参数的估计,研究结果为牙科修复材料的研发提供参考。

关键词: 牙釉质; 弹性常数; 力学参数; 超声共振谱; 共振频率
中图分类号: R 318.01 **文献标志码:** A
DOI: 10.16156/j.1004-7220.2017.05.009

Mechanical properties of human enamel based on resonant ultrasound spectroscopy

FENG Dan-dan, FAN Fan, WANG Rui, ZHANG Qiang, NIU Hai-jun(*School of Biological Science and Medical Engineering, Beihang University, Beijing* 100191, *China*)

Abstract: Objective To investigate the mechanical properties of human enamel based on resonant ultrasound spectroscopy (RUS). **Methods** The rectangular parallelepiped specimens of human enamel were processed. The theoretical resonant frequencies of specimens were estimated and paired with the experimental resonant frequencies measured from RUS experiments. An iterative procedure was used to adjust elastic constants of enamel until the theoretical frequencies corresponded to the experimental frequencies based on minimum mean-squared error criterion. In addition, elastic modulus, shear modulus and Poisson's ratio were calculated respectively. **Results** The elastic modulus, shear modulus and Poisson's ratio ranged from 61.52 to 80.46 GPa, 21.51 to 51.86 GPa and 0.18 to 0.43, respectively. Eliminating the effect of large specimen variances, the average of elastic modulus, shear modulus and Poisson's ratio was 72.84 GPa, 31.94 GPa and 0.27, respectively. **Conclusions** RUS performs a feasibility of measuring the mechanical properties of human enamel with repeatable and nondestructive advantages. All the elastic constants and mechanical parameters can be estimated through a signal experiment. The results provide references for the development of biomimetic dental restoration materials.

Key words: Enamel; Elastic constant; Mechanical parameter; Resonant ultrasound spectroscopy (RUS); Resonant frequency

人类牙齿主要由牙釉质、牙本质和牙髓构成,其中牙釉质的组成成分是无机物(主要为羟基磷灰石,占质量比96%~97%)、少量有机物和水。牙釉质覆盖在牙冠表面,起着保护内层组织的作用,是人

收稿日期: 2017-01-04; **修回日期:** 2017-03-10
基金项目: 国家自然科学基金项目(31570945),国家科技支撑计划项目(2015BAI06B02)。
通信作者: 牛海军,教授,博士研究生导师,E-mail: hjniu@buaa.edu.cn。

体钙化程度最高的硬组织[1]。牙釉质一旦磨损或损坏不可再生[2]，必须使用替代材料对其进行修补或重建。牙釉质的结构和功能与其材料的力学特性密切相关。

牙釉质力学特性测量的方法主要包括宏观拉伸[3-5]与压缩测试法[6-9]、声学法[10-12]与微观纳米压痕法[1-2,13-16]。这些方法促进了对牙釉质宏观与微观力学特性的理解，对牙科修复材料的研制、设计、制备与临床评价具有重要意义。然而，上述方法都存在一定缺陷，例如：宏观测试方法要求有较大体积的测试样本，且对牙釉质这种脆性材料很难进行重复测量；声学法虽是无损测量，但受波长影响，同样要求较大体积的测试样本；纳米压痕法可以用于测量小尺寸组织不同方向的弹性模量，但其主要反映微结构的力学性质，与宏观力学特性有明显差异。一直以来，研究报道的牙釉质力学特性测量值范围较大，为 24 ~ 96 GPa[4-7]。

品质因数 Q 是在拉伸、剪切、体积压缩、纵向压缩中测量得到的储能模量与损耗模量之比，是弹性材料的一个重要参数；Q 值愈大，说明材料变形中储能占比愈大，材料愈接近理想弹性。超声共振谱（resonant ultrasound spectroscopy，RUS）是20世纪90年代发展起来的一种表征材料特性的新方法[17-18]。其基本原理为运用超声激励样本产生自由振动，以获得包含样本多个固有频率的共振谱，然后结合数学反演方法推导出材料的弹性常数。该方法被物理学家认为是测量高 Q 值固体材料弹性常数的最准确方法[18]，可用于尺寸极小样本（< 1 mm）的多个弹性常数的无损测量，结果具有高度的可重复性。近年来，有研究将 RUS 应用于骨材料弹性常数测量，打破了 RUS 对于低 Q 值材料弹性常数测量的限制[19-21]。

本文基于 RUS 方法研究牙釉质材料的力学性质；通过提取人牙釉质材料的弹性常数，计算得到牙釉质材料的弹性模量、剪切模量和泊松比等力学参数，并与前人的研究结果进行对比。

1 实验和方法

基于 RUS 的样本弹性常数和力学参数计算方法主要包括3个步骤：① 根据所测物质的样本信息和先验知识假设的初始弹性常数，计算得到样本的理论共振频率；② 通过 RUS 实验测量并提取得到样本的实际共振频率；③ 基于均方误差最小准则（理论共振频率与实验测量频率之间的均方误差最小），通过迭代方法调整初始弹性常数，得到其最优估计，最后计算工程力学参数（见图1）。

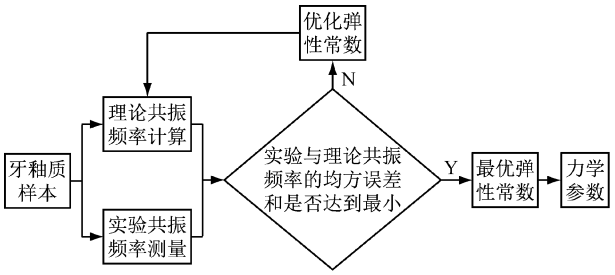

图1 RUS 方法流程图

Fig. 1 Flow chart of RUS

1.1 实验系统

实验系统由3部分组成：超声探头夹持器、振动信号放大与接收设备、力学参数计算设备。其中，超声探头为超声剪切波探头（V154RM，Panametrics Inc.，美国），信号放大与接收部分主要设备为电荷放大器（HQA-15M-10T，Femto Messtechnik GmbH，德国）和矢量网络分析仪（Bode 100，Omicron electronics GmbH，澳大利亚），共振谱分析和力学参数计算在计算机上进行［见图2（a）］。

1.2 样本制备

5颗磨牙样本，提供者为青年女性，年龄（26 ± 1）岁，基本信息如表1所示。

表1 牙釉质样本信息

Tab. 1 Size and quality of the enamel specimens

样本编号	长度/mm	宽度/mm	厚度/mm	质量/mg
1	3.443	3.353	1.653	52
2	3.683	3.040	1.660	51
3	3.070	1.980	1.867	31
4	3.240	2.120	1.647	30
5	2.956	1.880	1.672	24

首先剔除牙齿表面黏附的牙垢、肉芽等组织并清洗干净，然后用 SYJ-150 低速金刚石切割机（精度 0.01 mm）和全烧结金刚石锯片（厚 0.3 mm），在喷水状态下初步切割出磨牙的尖端牙釉质［见图2（b）］；分别使用500、800、2 000目砂纸对切割下来的样本块进行打磨，用于实验的样本块为标准长方

体,测量前将样本常温保存于生理盐水中,以保证样本处于潮湿状态。

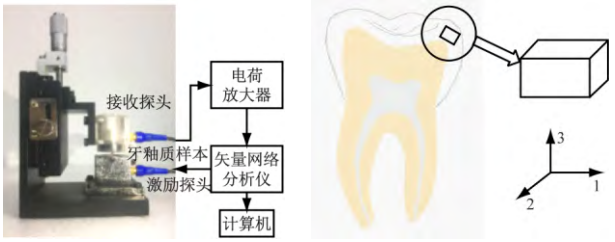

(a) 超声共振测量实验 (b) 牙釉质样本取样

图 2 实验平台与样本取样示意图

Fig. 2 Platform of RUS and sampling of specimen

(a) Experiment of RUS, (b) Sampling of enamel specimen

1.3 共振频率测量

实验时,将牙釉质样本对角放置于两个超声探头之间,按照图 2(a)所示线路连接设备。依据样本尺寸设置扫频范围和采样点数,分辨率保持在 100 Hz左右,扫频范围约包含前 30 阶共振频率[18]。对每个牙釉质样本进行 6 次独立扫描。图 3 所示为牙釉质样本的典型频谱,可以明显看到样本的共振峰;通过对共振峰的检测可获得样本的共振频率。

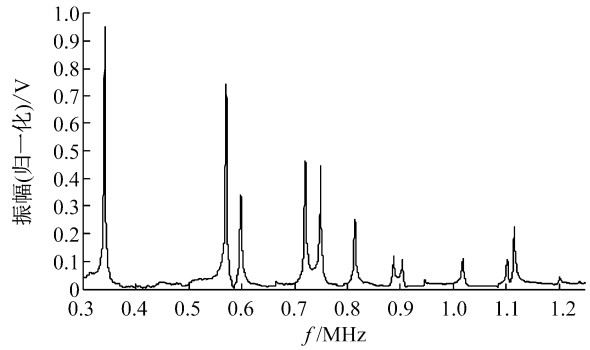

图 3 牙釉质样本典型共振频谱图

Fig. 3 Typical resonance spectrum of the enamel specimen

对每个牙釉质样本进行 6 次测量及共振频率提取后,可获得 6 组共振频率,选取其中至少出现 2 次的频率,计算其均值、标准差及变异系数(变异系数=标准差/均值×100%);选取其中标准差小于 1.5 且变异系数小于 0.3% 的频率均值作为相应频段上的实验共振频率。

1.4 理论共振频率计算

假设牙釉质样本为横观各向同性材料,则其具有 5 个独立的弹性常数:

$$\boldsymbol{C}_{ij}=\begin{pmatrix} C_{11} & C_{12} & C_{13} & 0 & 0 & 0 \\ C_{12} & C_{11} & C_{13} & 0 & 0 & 0 \\ C_{13} & C_{13} & C_{33} & 0 & 0 & 0 \\ 0 & 0 & 0 & C_{44} & 0 & 0 \\ 0 & 0 & 0 & 0 & C_{44} & 0 \\ 0 & 0 & 0 & 0 & 0 & \frac{1}{2}(C_{11}-C_{12}) \end{pmatrix} \tag{1}$$

式中:$C_{11}=82.96$ GPa;$C_{12}=36.04$ GPa;$C_{13}=34.66$ GPa;$C_{33}=92.89$ GPa;$C_{44}=22.90$ GPa[22]。

如果给定式(1)中的弹性常数 C_{ij},则可以利用寻找拉格朗日方程 L 驻点的方法获得牙釉质样本的理论共振频率:

$$L=\frac{1}{2}\int_V\left[\rho(2\pi f)^2u_i^2-C_{ijkl}\frac{\partial u_i}{\partial x_j}\frac{\partial u_k}{\partial x_l}\right]\mathrm{d}V \tag{2}$$

式中:ρ 和 V 分别为牙釉质样本的密度和体积;C_{ijkl}为牙釉质的初始弹性常数;f 为牙釉质的共振频率;u 为位移场,一般采用瑞利里兹法(Rayleigh-Ritz)进行求解;f 的具体计算过程见文献[23]。

1.5 力学常量提取

通过上述方法分别获得牙釉质样本实验和理论共振频率后,首先定义目标函数

$$F(C)=\sum_{i=1}^{n}w_i(f_i^{\exp}-f_i^{\mathrm{cal}}(C))^2 \tag{3}$$

式中:n 为实验共振频率个数;C 为牙釉质的弹性常数;f_i^{cal} 为第 i 个理论共振频率;$f_i^{\exp}$ 为第 i 个实验共振频率;w_i 为权重,即

$$w_i=\begin{cases}0, & \text{若无与 } f_i^{\mathrm{cal}} \text{ 对应的 } f_i^{\exp}\\ 1/(f_i^{\exp})^2, & \text{若有与 } f_i^{\mathrm{cal}} \text{ 对应的 } f_i^{\exp}\end{cases} \tag{4}$$

采用列文伯格优化算法(Levenberg-Marquardt,LM)[24],通过迭代计算,求取 $F(C)$ 的最小值。在收敛条件下,$F(C)$ 达到最小时的 C 即为所测量样本的弹性常数。

根据广义胡克定律,横观各向同性材料的弹性常数与工程力学参数之间的关系为:

$$C_{ij}^{-1}=\begin{pmatrix} 1/E_{11} & -\nu_{12}/E_{11} & -\nu_{13}/E_{11} & 0 & 0 & 0 \\ -\nu_{12}/E_{11} & 1/E_{11} & -\nu_{13}/E_{11} & 0 & 0 & 0 \\ -\nu_{13}/E_{11} & -\nu_{13}/E_{11} & 1/E_{33} & 0 & 0 & 0 \\ 0 & 0 & 0 & 1/G_{13} & 0 & 0 \\ 0 & 0 & 0 & 0 & 1/G_{13} & 0 \\ 0 & 0 & 0 & 0 & 0 & 1/G_{12} \end{pmatrix} \tag{5}$$

式中: E_{11}、E_{33} 分别为沿弹性方向 1、3 的弹性模量; G_{13}、G_{12} 分别为决定 1-3、1-2 平面内的剪切模量; ν_{12}、ν_{13} 分别为对应方向上的泊松比。其中,E_{11} = 62.40 GPa,E_{33} = 72.70 GPa,ν_{12} = 0.33,ν_{13} = 0.25,G_{13} = 22.90 GPa,G_{12} = 24.80 GPa[22]。

2 结果

通过 LM 算法对目标函数 $F(C)$ 进行优化。表 2 所示为优化结束后,最优弹性常数基础上计算得到的理论与实验共振频率的典型配对表(以样本 3 为例)。几乎每一个理论共振频率都有与之相匹配的实验共振频率,表中虚线则表示在频谱中未找到能够与理论共振频率相匹配的实验共振频率,优化时按照式(4)将其权重置为 0,即忽略不计。计算已配对共振频率的相对误差,其绝对值均小于0.7%,满足小于 0.8% 的要求[18]。

表 2 LM 优化后理论共振频率与实验共振频率配对表

Tab. 2 Pair comparison of experiment frequencies with calculated frequencies after optimization

	实验共振频率/kHz	理论共振频率/kHz	相对误差%		实验共振频率/kHz	理论共振频率/kHz	相对误差%
1	341.927	343.036	0.324	13	905.234	904.520	-0.079
2	571.081	570.524	-0.097	14	947.591	950.057	0.260
3	599.219	601.952	0.456	15	962.266	963.896	0.169
4	646.927	645.204	-0.266	16	1 018.75	1 014.894	-0.378
5	666.641	667.028	0.058	17	—	1 038.784	—
6	—	701.501	—	18	1 086.09	1 084.817	-0.118
7	720.755	717.074	-0.511	19	1 102.53	1 109.526	0.634
8	749.492	752.085	0.346	20	1 116.24	1 123.475	0.648
9	—	796.523	—	21	—	1 173.934	—
10	814.831	810.449	-0.538	22	—	1 178.478	—
11	830.566	832.903	0.281	23	1 201.41	1 196.124	-0.440
12	887.279	884.137	-0.354	24	1 238.77	1 240.120	0.109

5 个牙釉质样本的弹性常数见表 3,其中 C_{11}、C_{12}、C_{13}、C_{33}、C_{44} 范围分别为: 84.80 ~ 96.63 GPa,26.30 ~ 49.62 GPa,23.41 ~ 58.01 GPa,69.67 ~ 94.13 GPa,27.33 ~ 55.94 GPa。

表 3 牙釉质样本的弹性常数

Tab. 3 Elastic constants of the enamel specimens

样本	C_{11}/GPa	C_{12}/GPa	C_{13}/GPa	C_{33}/GPa	C_{44}/GPa
1	88.50	49.62	58.01	69.67	55.94
2	92.04	26.30	32.68	94.13	29.65
3	96.72	43.46	23.41	72.32	51.86
4	96.63	30.53	31.89	83.57	32.61
5	84.80	41.79	29.56	93.78	27.33

表 4 所示为 5 个牙釉质样本的力学参数,其中样本 1 的结果与其他样本结果具有较大差异。排除样本 1 后,E_{11}、E_{33} 范围分别为: 61.52 ~ 80.46 GPa,64.50 ~ 79.98 GPa; ν_{12}、ν_{13} 范围分别为: 0.18 ~ 0.43,0.18 ~ 0.30; G_{13}、G_{12} 范围分别为: 27.33 ~ 51.86 GPa,21.51 ~ 33.05 GPa。

表 4 牙釉质样本的力学参数

Tab. 4 Mechanical parameters of the enamel specimens

样本	E_{11}/GPa	E_{33}/GPa	ν_{12}	ν_{13}	G_{13}/GPa	G_{12}/GPa
1	40.16	20.95	0.03	0.81	55.94	19.44
2	77.92	76.08	0.18	0.28	29.65	32.87
3	74.69	64.50	0.40	0.19	51.86	26.63
4	80.46	67.57	0.22	0.30	32.61	33.05
5	61.52	79.98	0.43	0.18	27.33	21.51

3 讨论

由于具有高度的重复一致性和测量准确性等特点,RUS 方法已被用于晶体、金属与复合材料的力学特性测量[23]。近年来,一些研究打破了该方法难以测量低 Q 值材料的限制,将其应用拓展到了生物

材料领域[19-20]。本文基于RUS方法测量并计算了人牙釉质材料的弹性常数与力学参数。

牙齿材料的弹性属性是牙齿强度研究中最受关注和最重要的性质,主要包括弹性模量、剪切模量和泊松比。弹性常数(表征材料弹性的量)通常由刚度矩阵和柔性矩阵定义,根据材料的微结构和对称性,独立弹性常数的个数不同;因此,研究牙齿的弹性属性必须考虑材料的对称性。例如,各向同性材料只有2个独立的弹性常数,正交各向异性材料有9个独立常数,而单对称材料有13个独立常数。本文假设牙釉质材料为横观各向同性材料,其具有5个独立的弹性常数 C_{11}、C_{12}、C_{13}、C_{33}和 C_{44}。

有关牙齿材料力学特性的研究,曾采用过拉伸法、压缩法、弯曲法、超声声速法、电阻应变片法等多种测量方法获取牙齿的弹性模量,但测量得到的弹性模量数值非常不一致。牙本质弹性模量的数值为2~30 GPa[9,26-30]。牙釉质弹性模量的测量值差异同样较大。叶德临等[4]采用拉伸法获得的人磨牙牙釉质的弹性模量为24.9~26.8 GPa,泊松比为0.15~0.36[5]。Stanford等[6]测得尖端牙釉质的弹性模量均值为56.5 GPa。Craig等[7]利用压缩法得到人牙釉质的弹性模量为62.74~95.84 GPa。本文基于RUS方法测量得到牙釉质样本的弹性模量为61.52~80.46 GPa,剪切模量为21.51~51.86 GPa,泊松比为0.18~0.43。在所有测量样本中,第1块样本的数值明显区别于其他样本,推测是样本体积较大,样本中夹杂了少量牙本质,或者样本中间有部分微小缺陷造成的。如果不考虑样本1的测量值,则平均弹性模量、剪切模量和泊松比分别为72.84 GPa、31.94 GPa和0.27,该测量结果与Craig等[7]的结果基本一致。

由于RUS测量方法的准确性与重复一致性已被证明,故本文更侧重于认为牙釉质材料应该具有较大的弹性模量。前人测量得到的数值较小,推测原因如下:① 牙釉质样本不容易制作,样本中夹杂有牙本质材料,而牙本质明显比牙釉质的弹性模量小[6,9,31],或者样本存在着微小缺损。Craig等[7]也曾指出,测量结果值低的原因可能源于样本自身的干扰。② 采用拉伸和压缩等机械测量方法时,由于样本尺寸很小,对样本的夹持会造成较大测量误差。③ 牙釉质取样位置不同也可能影响测量结果。

本研究的局限性如下:① 天然的牙釉质材料为非均质、各向异性材料[13],而本文假设其为横观各向同性材料,测量结果会存在一定误差。由于目前RUS方法需要使用高度规则的测试样本,而牙釉质为脆性材料且体积较小,加工规则体样本产生的误差对最终结果会产生一定影响。② 所采用的样本较少,下一步研究需要增加样本量。本文研究结果证明了RUS方法在测量牙釉质力学特性方面的可行性。

参考文献:

[1] LI HH, SWAIN MV. Understanding the mechanical behaviour of human enamel from its structural and compositional characteristics [J]. J Mech Behav Bio Mater, 2008, 1(1): 18-29.

[2] CUY JL, MANN AB, LIVI KJ, *et al*. Nanoindentation mapping of the mechanical properties of human molar tooth enamel [J]. Arch Oral Biol, 2002, 47(4): 281-291.

[3] BOWEN RL, RODRIGUEZ MS. Tensile strength and modulus of elasticity of tooth structure and several restorative materials [J]. J Am Dent Assoc, 1962, 64(3): 378-387.

[4] 叶德临, 向云乡, 张尚慧, 等. 电阻应变测试技术测人牙釉质的弹性模量 [J]. 华西口腔医学杂志, 1991, 9(3): 207-209.

[5] 叶德临, 苏玉瑞, 王彬, 等. 人牙釉质泊松比的测定 [J]. 华西口腔医学杂志, 1994, 12(4): 295-297.

[6] STANFORD JW, PAFFENBARGER GC, KUMPULA JW, *et al*. Determination of some compressive properties of human enamel and dentin [J]. J Am Dent Assoc, 1958, 57(4): 487-495.

[7] CRAIG RG, PEYTON FA, JOHNSON DW. Compressive properties of enamel, dental cements, and gold [J]. J Dent Res, 1961, 40(5): 936-945

[8] STAINES M, ROBINSON WH, HOOD JAA. Spherical indentation of tooth enamel [J]. J Mater Sci, 1981, 16(9): 2551-2556.

[9] CHUN K, CHOI H, LEE J. Comparison of mechanical property and role between enamel and dentin in the human teeth [J]. J Dent Biomech, 2014, doi: 10.1177/1758736014520809.

[10] GILMORE RS, POLLACK RP, KATZ JL. Elastic properties of bovine dentine and enamel [J]. Arch Oral Biol, 1970, 15(8): 787-796.

[11] GRENOBLE DE, KATZ JL, DUNN KL, *et al*. The elastic properties of hard tissues and apatites [J]. J Biomed Ma-

ter Res, 1972, 6(3): 221-233.

[12] NG SY, PAYNE PA, CARTLEDGE NA, *et al*. Determination of ultrasonic velocity in human enamel and dentine [J]. Arch Oral Biol, 1989, 34(5): 341-345.

[13] ZHANG YR, DU W, ZHOU XD, *et al*. Review of research on the mechanical properties of the human tooth [J]. Int J Oral Sci, 2014, 6(2): 61-69.

[14] HABELITZ S, MARSHALL SJ, MARSHALL GW, *et al*. Mechanical properties of human dental enamel on the nanometre scale [J]. Arch Oral Biol, 2001, 46(2): 173-183.

[15] ZHOU J, HSIUNG LL. Depth dependence of the mechanical properties of human enamel by nanoindentation [J]. J Biomed Mat Res A, 2006, 81A(1): 1-28

[16] HE LH, FUJISAWA N, SWAIN MV. Elastic modulus and stress-strain response of human enamel by nano-indentation [J]. Biomaterials, 2006, 27(24): 4388-4398.

[17] MIGLIORI A, SARRAO JL, VISSCHER WM, *et al*. Resonant ultrasound spectroscopic techniques for measurement of the elastic moduli of solids [J]. Phys B, 1993, 183(1-2): 1-24.

[18] MIGLIORI A, MAYNARD JD. Implementation of a modern resonant ultrasound spectroscopy system for the measurement of the elastic moduli of small solid specimens [J]. Rev Sci Instrum, 2005, 76(12), doi: http://dx.doi.org/10.1063/1.2140494.

[19] BERNARD S, GRIMAL Q, HAUPERT S, *et al*. Assessment of anisotropic elasticity of small bone samples with resonant ultrasound spectroscopy: Attenuation does not prevent the measurements [C]// Proceedings of International Ultrasonics Symposium. Orlando: IEEE, 2011: 1599-1602.

[20] BERNARD S, GRIMAL Q, LAUGIER P. Accurate measurement of cortical bone elasticity tensor with resonant ultrasound spectroscopy [J]. J Mech Behav Bio Mater, 2013, 18C: 12-19.

[21] BERNARD S, GRIMAL Q, LAUGIER P. Measuring viscoelastic properties of cortical bone with resonant ultrasound spectroscopy [C]//Proceedings of International Ultrasonics Symposium. Dresden: IEEE, 2012: 1-4.

[22] 文鸣，郑靖，周仲荣. 有机相对人牙釉质力学性能影响的有限元分析 [J]. 润滑与密封，2014，39(7)：21-25.

[23] MIGLIORI A, SARRAO JL. Resonant ultrasound spectroscopy: Applications to physics, materials measurements, and nondestructive evaluation [M]. New York: Wiley, 1997.

[24] BERNARD S, GRIMAL Q, LAUGIER P. Resonant ultrasound spectroscopy for viscoelastic characterization of anisotropic attenuative solid materials [J]. J Acous Soc Am, 2014, 135(5): 2601-2613.

[25] Schwarz RB, Vuorinen JF. Resonant ultrasound spectroscopy: Applications, current status and limitations [J]. J Alloys Compounds, 2000, 310(1): 243-250.

[26] 王文亚，傅波，罗华，等. 不同桩核冠修复上颌中切牙的三维有限元模型建立及应力分析 [J]. 医用生物力学，2014，29(1)：25-30.
WANG WY, FU B, LUO H, *et al*. Three-dimensional finite element modeling and stress analysis on different posts and cores for repairing the maxillary central incisors [J]. J Med Biomech, 2014, 29(1): 25-30.

[27] BO H, ZHENG Q. Effect of dentin tubules to the mechanical properties of dentin. Part II: Experimental study [J]. Acta Mechan Sinica, 2000, 16(1): 75-82.

[28] KISHEN A, RAMAMURTY U, ASUNDI A. Experimental studies on the nature of property gradients in the human dentine [J]. J Biomed Mater Res, 2000, 51(4): 650-659.

[29] KINNEY JH, OLIVEIRA J, HAUPT DL, *et al*. The spatial arrangement of tubules in human dentin [J]. J Mater Sci Mater Med, 2001, 12(8): 743-751.

[30] 刘旺玉，吴华锋，蔡斌. 牙周膜厚度对舌侧矫治中下颌第1磨牙近中移动的影响 [J]. 医用生物力学，2013，28(2)：223-228.
LIU WY, WU HF, CAI B. Effects of periodontal ligament thickness on mesial movement of mandibular first molar in lingual orthodontics [J]. J Med Biomech, 2013, 28(2): 223-228.

[31] 葛俊，崔福斋，吉宁，等. 人牙釉质分级结构的观察 [J]. 牙体牙髓牙周病学杂志，2006，16(2)：61-66.

Hindawi
BioMed Research International
Volume 2017, Article ID 7852971, 7 pages
https://doi.org/10.1155/2017/7852971

Research Article

The Elasticity Coefficients Measurement of Human Dentin Based on RUS

Fan Fan, Dandan Feng, Rui Wang, Qiang Zhang, and Haijun Niu

Key Laboratory of Ministry of Education for Biomechanics and Mechanobiology, School of Biological Science and Medical Engineering, Beihang University, Beijing, China

Correspondence should be addressed to Haijun Niu; hjniu@buaa.edu.cn

Received 4 November 2016; Accepted 5 April 2017; Published 30 April 2017

Academic Editor: Andrea Scribante

This paper proposed to take advantages of resonant ultrasound spectroscopy (RUS) to measure the mechanical properties of human dentin specimen. The resonant spectroscopy of the dentin specimen was obtained between the frequency bands 155 and 575 kHz, and resonant frequencies were extracted by linear predictive filter and then by Levenberg-Marquardt method. By inverse problem approach, 13 experimental resonant frequencies progressively matched to the first 30 orders of theoretical resonant frequencies calculated by Lagrangian variational method. The full second-order elastic tensor of dentin specimen was adjusted. The whole set of human dentin engineering moduli, including Young's moduli (E_{11} = 22.641 GPa, E_{33} = 13.637 GPa), shear moduli (G_{12} = 10.608 GPa, G_{23} = 7.742 Gpa), and Poisson's ratios (ν_{12} = 0.067, ν_{31} = 0.378), were finally calculated. This study demonstrates that RUS can be successfully adapted to measure the mechanical properties of low quality factor biomaterials.

1. Introduction

As the most abundant mineralized tissue in human teeth, dentin is composed of about 50% inorganic components (basically calcium hydroxyapatite), 30% organic components (mainly type I collagen fibers), and 20% water [1, 2]. Compared with enamel, dentin has less inorganic components and thus is softer and more elastic. These characteristics ensure dentin being indispensable to cushion chewing force and protect internal pulp [3].

The researches about dentin mechanical properties began from 19th century and never stopped since then [3]. To date, the main methods of dentin mechanical properties measurement mainly included tensile and compression test [2, 4], acoustics method (pulse echo method, bulk wave method, elasticity imaging, etc.) [4–8], and macroscopic indentation and nanoindentation method [9–11]. These methods helped not only promote the understanding of macromechanical properties of dentin and micromechanical properties of dentin tubule, but offer important significance for the design, development, and evaluation of clinical dental restorative materials as well. Nevertheless, these methods mentioned above have their own limitations. For example, the macrotest methods required a relative larger size of the specimen, which was difficult to obtain from human dentin. Besides, although the nanoindentation method could be used to measure the elastic moduli in different directions of small-sized specimen, it mainly reflected that the mechanical properties deeply rely on the scope of indentation, which led to the differences from the macroscopic mechanical properties.

Since the 1990s, resonant ultrasound spectroscopy (RUS) has been developed as an accurate and efficient method to characterize the material properties [12–15]. The basic mechanism of RUS is to obtain a series of mechanical resonant frequencies by generating free vibrations with ultrasound excitations, then predict theoretical model frequencies with Lagrangian variational method, and finally get the material elastic properties by comparing the measured frequencies with the predicted ones (inverse problem approach). RUS has been regarded as the gold standard for measuring the elastic moduli of high Q (quality factor) solid materials. And it beats other methods by the following three advantages: ① The full elastic tensor could be assessed from a single sample in a single nondestructive experiment over other elasticity measurement methods; ② RUS was well-adapted to small-sized samples (a few millimeters or less); ③ The measurement results

were more repeatable and accurate [12, 14, 16]. In recent years, Pascal's group were dedicated to measuring the elastic coefficients of cortical bone by RUS, which made it possible for breaking the limitations when measuring low-Q materials by RUS [12, 13, 17].

In this paper, the method of human dentin elasticity extraction based on RUS was studied. Firstly, the resonant spectroscopy of dentin specimen was obtained by ultrasound experiment. Then, the resonant frequencies were extracted through signal processing of linear predictive filter and then by nonlinear least squares method (Levenberg-Marquardt method). Combined with the theoretical resonant frequencies calculated by Lagrangian variational method, inverse problem approach was introduced to obtain the complete second-order elastic tensor of dentin samples. The engineering moduli, including Young's moduli, shear moduli, and Poisson's ratios, were finally calculated.

2. Materials and Methods

2.1. Specimen Preparations. The tooth used in this paper was complete, fresh, and caries-free. It was a left upper third molar from a 25-year-old male, which was collected from Beihang Hospital. The donor provided consent to donate his tooth for this study. The entire experimental procedures were approved by the Institutional Animal Care and Use Committee of Beihang University and performed under the guidelines of the National Institutes of Health.

Before experimentation began, the specimen was stored in saline solution at room temperature (22°C). After cleaning the entire tooth surface by removing calculus and granulation, the dentin part was cut into a rectangular parallelepiped by a low speed diamond cutting machine (SYJ-150, Shenyang Kejing Auto-Instrument Co., Ltd., Shenyang, China) with 0.01 mm positioning accuracy and 25–300 rad/min rotational speed and a whole sintered diamond saw blade (0.3 mm thick). The six faces of the specimen were polished with P500, P800, and P1000 abrasive paper progressively. With repeated protractor measurements of each corner of the specimen and polish, a standard rectangular parallelepiped human dentin specimen was obtained (accuracy: $90^\circ \pm 0.5^\circ$) [12]. The mass of the specimen was 111 mg, and the dimensions were 5.696 mm × 3.620 mm × 2.704 mm.

2.2. Theoretical Resonant Frequencies Calculation. The resonant frequencies of solid material are related to many factors such as density, dimensions, elastic tensor, and boundary conditions. Moreover, the relationship among these factors is nonlinear and no analytical solutions exist either. To figure out the approximate numerical solutions, Lagrange variational method was imported here. As (1) shows, the resonant angular frequencies ω could be calculated by searching for the stationary points of the Lagrangian L under free-surface boundary condition [14, 18–21].

$$L = \int \left(E_k - E_p\right) dV, \tag{1}$$

where E_k and E_p are kinetic energy and potential energy, respectively, given by

$$E_k = \frac{1}{2}\sum_i \rho\omega^2 {u_i}^2,$$
$$E_p = \frac{1}{2}\sum_{i,j,k,l} c_{ijkl}\frac{\partial u_i}{\partial x_j}\frac{\partial u_k}{\partial x_l}. \tag{2}$$

In (2), ρ and V are the specimen's density and volume, respectively, u_i is the component of the displacement field in Cartesian coordinates, and c_{ijkl} are the stiffness constants of solid material.

Kinney et al. found the elastic constants C_{ij} of hydrated dentin exhibited as transverse isotropy, with five independent constants: C_{11}, C_{12}, C_{13}, C_{33}, and C_{44}, as (3) shows [1, 22]:

$$C_{ij} = \begin{pmatrix} C_{11} & C_{12} & C_{13} & 0 & 0 & 0 \\ C_{12} & C_{11} & C_{13} & 0 & 0 & 0 \\ C_{13} & C_{13} & C_{33} & 0 & 0 & 0 \\ 0 & 0 & 0 & C_{44} & 0 & 0 \\ 0 & 0 & 0 & 0 & C_{44} & 0 \\ 0 & 0 & 0 & 0 & 0 & \frac{1}{2}\left(C_{11} - C_{12}\right) \end{pmatrix}. \tag{3}$$

To find the stationary point of the Lagrangian L, (4) was calculated:

$$\delta L = 0. \tag{4}$$

To solve the numerical solutions of (4), by expanding the displacement field u_i to a set of polynomial functions, Rayleigh-Ritz method was introduced:

$$u_i = \sum_\lambda a_{i\lambda}\phi_\lambda, \tag{5}$$

where the choice of ϕ_λ is rather arbitrary.

Historically, Visscher et al. found that there was none simpler than powers of the Cartesian coordinates when expanding the displacement field [18], so a set of power exponent functions were chosen for simplifying computing:

$$\phi_\lambda = x^l y^m z^n, \tag{6}$$

where $l + m + n \le N$.

When $N \to +\infty$, the solutions of (4) are the exact solutions. Considering a good compromise between computational accuracy and computing time, N was chosen as 12.

Based on (5) and (6), (4) was transferred to the generalized eigenvalue problem:

$$\omega^2 Ea = \Gamma a, \tag{7}$$

where E and Γ are expressed as follows:

$$E_{\lambda i\lambda' i'} = \delta_{ii'}\rho\int_V x^{l+l'} y^{m+m'} z^{n+n'} dV,$$
$$\Gamma_{\lambda i\lambda' i'} = \sum_{j,j'} C_{iji'j'}\int_V \frac{\partial x^l y^m z^n}{\partial x_j}\frac{\partial x^{l'} y^{m'} z^{n'}}{\partial x_{j'}} dV. \tag{8}$$

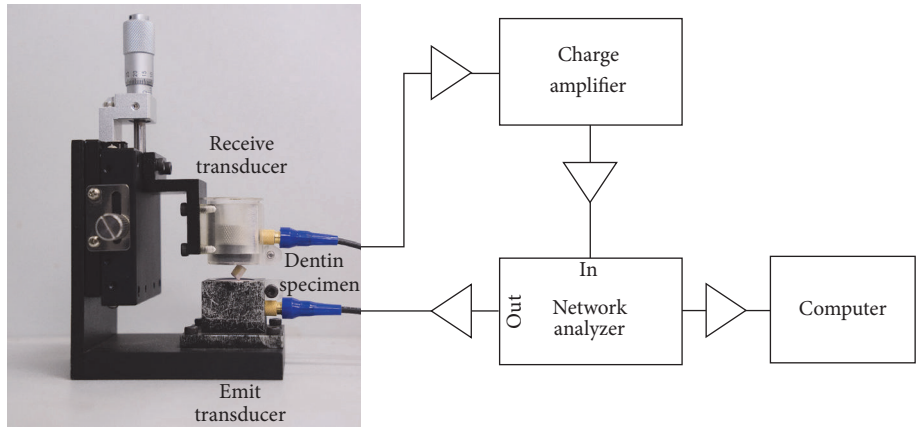

Figure 1: RUS experiment platform: photograph of the dentin specimen mounted between emitting and receiving transducers and block diagram of other hardware.

In the end, the theoretical values of solid resonant frequency could be calculated by solving (7).

Before the resonance experiment, a set of initial elastic tensors combined with the density and dentin specimen dimensions were needed to be set; then the theoretical resonant frequencies could be calculated later. The initial elastic tensor set plays a decisive role in iterative efficiency and accuracy, so it is indispensable to find an exact-value-closest set as shown in matrix (9) [18, 22]. In this paper, the first 30 frequencies' range was chosen as the experimental frequency sweep range reference.

$$\begin{pmatrix} 42.6 & 25.4 & 19.7 & 0 & 0 & 0 \\ 25.4 & 42.6 & 19.7 & 0 & 0 & 0 \\ 19.7 & 19.7 & 34.6 & 0 & 0 & 0 \\ 0 & 0 & 0 & 9.4 & 0 & 0 \\ 0 & 0 & 0 & 0 & 9.4 & 0 \\ 0 & 0 & 0 & 0 & 0 & 8.6 \end{pmatrix}. \tag{9}$$

2.3. RUS Experiment. The RUS experiment platform is shown in Figure 1. The platform was made just to fit the free-surface boundary condition. The dentin specimen was mounted on opposing corners between two shear wave contact transducers (V154RM, Panametrics Inc., Waltham, US) in the RUS system. A network analyzer (Bode 100, Omicron electronics GmbH, Klaus, Austria) was used to output a swept-frequency signal between 155 kHz and 575 kHz (frequency resolution: 30 Hz) as the excitation of the transmit transducer. The frequency response of the specimen was received by the other transducer, amplified by a broadband charge amplifier (HQA-15M-10T, Femto Messtechnik GmbH, Berlin, Germany), sent back to the network analyzer, and recorded [12].

2.4. Experimental Resonant Frequencies Extraction. The frequency response FR acquired by the network analyzer was modeled as a sum of M Lorentzian lineshapes [12]:

$$\mathrm{FR}(f) = \sum_{k=1}^{M} \frac{a_k}{\left(f_k{}^2 - f^2\right) + i\left(f_k f / Q_k\right)}, \tag{10}$$

where a_k are the complex amplitudes, f_k are the resonant frequencies, and Q_k are the resonant quality factors.

When RUS was used on low damping (high Q) materials, the resonant frequencies f_k, the sharp peak, could be easily recognized from the resonant spectrum. For those low Q materials such as dentin, peaks may be broad and overlap each other, which made it difficult to directly extract resonant frequencies from spectrum. Therefore linear predictive filter, an accurate signal processing method, introduced by Kumaresan, Tufts, and Lebedev et al. was selected here to distinguish the resonant frequencies, which was proved to be a perfect solution [23–27].

The frequency response FR was converted to $y(n)$ in time domain by N-point inverse Fourier transform (N is the length of the FR data), and then matrix A was created based on

$$A = \begin{pmatrix} y(L) & y(L-1) & \cdots & y(1) \\ y(L+1) & y(L) & \cdots & y(2) \\ \vdots & \vdots & \ddots & \vdots \\ y(N-1) & y(N-2) & \cdots & y(N-L) \end{pmatrix}. \tag{11}$$

According to the linear prediction method, the first L points of $y(n)$ contained enough information to predict values of the others. So the linear predictive filter equation could be set as

$$Ag = b, \tag{12}$$

where b has the definition:

$$b = \begin{pmatrix} y(L+1) \\ y(L+2) \\ \vdots \\ y(N) \end{pmatrix} \tag{13}$$

and g is a column vector with L components:

$$g = \begin{pmatrix} g_1 \\ g_2 \\ \vdots \\ g_L \end{pmatrix}. \tag{14}$$

Then the transfer function of this linear predictive filter could be written as

$$H(z) = 1 + \sum_{k=1}^{L} g_k z^{-k}. \tag{15}$$

The predicted values of the resonant frequency f_k and the quality factor Q_k could be obtained by finding the zeros outside the unit circle in Z domain. Substituting the predicted f_k and Q_k into (10), complex resonant amplitude a_k and also the predicted frequency spectrum FRlp could be calculated. One of the advantages of this method was that there was no need to know the exact numbers of resonant peaks in FR, but some differences existed between FRlp and FR. To figure out these differences, a Levenberg-Marquardt method was taken to optimize the parameters, and we considered the f_k's which minimized (16), the true resonant frequencies [28].

$$F(f) = \sum \left(\frac{\mathrm{FR}lp(f) - \mathrm{FR}(f)}{\mathrm{FR}(f)} \right)^2. \tag{16}$$

During a single experiment, some resonant mode might not be excited, so 7 measurements on the dentin specimen, by remounting it on opposing corners each time, were conducted for a good reproducibility. Each of the regarded experimental resonant frequencies f^{exp} was present in at least two frequency responses in the 7 measurements.

2.5. Elastic Tensor Calculation. Levenberg-Marquardt nonlinear optimization inverse problem approach was selected for the purpose of calculating the elastic tensor [14, 28, 29]. Here the cost function was introduced as a criterion for the iteration, and the value of the cost function was calculated, as shown in

$$F(C) = \sum_{i=1}^{N} w_i \left(f_i^{\mathrm{exp}} - f_i^{\mathrm{cal}}(C) \right)^2, \tag{17}$$

where C is an independent component of the elastic tensor, N is the number of the resonant frequency, f_i^{cal} is the ith order calculated resonance frequency, f_i^{exp} is the ith order experimental resonance frequency, and w_i is weighting factor, expressed as follows:

$$w_i = \begin{cases} 0 & f_i^{\mathrm{cal}} \text{ does not match } f_i^{\mathrm{exp}} \\ \dfrac{1}{\left(f_i^{\mathrm{exp}}\right)^2} & f_i^{\mathrm{cal}} \text{ matches } f_i^{\mathrm{exp}}. \end{cases} \tag{18}$$

The iterative process was completed when the experimental and theoretical frequencies matched perfectly. In other words, cost function reached the global minimum and also became convergent.

2.6. Engineering Moduli Calculation. The 6×6 stiffness matrix was constructed and numerically inverted to obtain the compliance matrix C_{ij}^{-1}, from which engineering moduli could be calculated.

$$C_{ij}^{-1} = \begin{pmatrix} \frac{1}{E_{11}} & \frac{-\nu_{12}}{E_{11}} & \frac{-\nu_{31}}{E_{33}} & 0 & 0 & 0 \\ \frac{-\nu_{12}}{E_{11}} & \frac{1}{E_{11}} & \frac{-\nu_{31}}{E_{33}} & 0 & 0 & 0 \\ \frac{-\nu_{31}}{E_{33}} & \frac{-\nu_{31}}{E_{33}} & \frac{1}{E_{33}} & 0 & 0 & 0 \\ 0 & 0 & 0 & \frac{1}{G_{23}} & 0 & 0 \\ 0 & 0 & 0 & 0 & \frac{1}{G_{23}} & 0 \\ 0 & 0 & 0 & 0 & 0 & \frac{1}{G_{12}} \end{pmatrix}, \tag{19}$$

where E_{ii}'s are Young's moduli (GPa), G_{ij}'s are shear moduli (GPa), and ν_{ij}'s are Poisson's ratios.

3. Result and Discussion

3.1. Results of Experimental Resonant Frequencies Extractions. In accordance with the method of 2.4, in each of 7 measurements, two or more resonant frequencies with similar Q values were selected, and their mean values and standard deviations were calculated from 2 to 7 values depending on the frequency. As shown in Table 1, when the standard deviation (column 2) was less than 0.5%, the mean value (column 1) was retained as the resonant frequencies extracted from the experiment.

Figure 2 shows the measured frequency responses of the dentin specimen between 155 and 575 kHz. The 16 calculated resonant frequencies, presented at least two times, are represented as $*$. The mean values are represented as the vertical line.

3.2. Results of the Inverse Problem. After nonlinear optimization, the theoretical values of resonant frequency were obtained and shown in column 4 of Table 2. Among the first 30 orders of the calculated resonant frequencies, 13 can be paired with the measured frequencies. The root-mean-square error between calculated and experimental frequencies was below 0.65%.

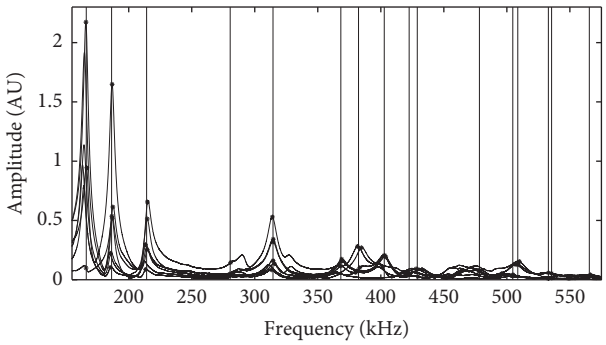

Figure 2: Measured frequency response of the dentin specimen between 155 and 575 kHz and the 16 resonant frequencies distributions. ∗: the calculated resonant frequencies presented at least two times. Vertical line: the mean values of the resonant frequencies.

Table 1: Results of 16 experimental resonant frequencies' extraction and Q factors.

f^{exp}/kHz	SD%	Q
166.34	0.22	45.56
186.44	0.43	46.05
214.20	0.36	45.40
280.50	0.20	47.98
314.47	0.22	42.05
368.28	0.23	46.41
382.30	0.45	44.57
402.73	0.29	48.32
422.47	0.17	46.21
428.92	0.19	40.78
478.22	0.18	44.81
504.72	0.06	42.28
508.66	0.25	45.63
532.94	0.01	53.49
535.48	0.02	39.95
565.41	0.22	48.76

The correspondence elastic tensor is shown in matrix (20), with the unit of GPa.

$$\begin{pmatrix} 35.27 & 14.06 & 18.63 & 0 & 0 & 0 \\ 14.06 & 35.27 & 18.63 & 0 & 0 & 0 \\ 18.63 & 18.63 & 27.71 & 0 & 0 & 0 \\ 0 & 0 & 0 & 7.74 & 0 & 0 \\ 0 & 0 & 0 & 0 & 7.74 & 0 \\ 0 & 0 & 0 & 0 & 0 & 10.61 \end{pmatrix}. \quad (20)$$

3.3. Results of Engineering Moduli Calculations. In accordance with (19), engineering moduli could be calculated as shown in Table 3. Column 3 also listed the engineering moduli results of Kinney et al.'s work [22].

3.4. Discussion. In this paper, the method of human dentin elasticity extraction based on RUS was studied. Firstly, the resonant spectroscopy between 155 and 575 kHz of a dentin specimen was obtained. The resonant frequencies were extracted by linear predictive filter and then by nonlinear least squares method (Levenberg-Marquardt method). Combined with the theoretical resonant frequencies calculated by Lagrangian variational method, inverse problem approach was introduced to obtain the complete second-order elastic tensor of the dentin sample. Young's moduli, shear moduli, and Poisson's ratios were finally calculated.

Table 2: Results of the original calculated, experimental, and optimized calculated resonant frequencies.

Mode	Original f^{cal}/kHz	f^{exp}/kHz	Final f^{cal}/kHz	Err%
1	161.13	166.34	165.53	−0.48
2	195.31	186.44	186.62	0.10
3	220.66	214.20	213.07	−0.53
4	292.13	280.50	281.66	0.42
5	294.42	—	312.63	—
6	313.36	314.47	313.06	−0.45
7	333.39	—	315.26	—
8	366.55	—	342.12	—
9	385.12	—	350.58	—
10	412.00	368.28	368.17	−0.03
11	414.05	—	370.08	—
12	416.61	382.30	384.59	0.60
13	418.61	—	386.37	—
14	438.89	402.73	401.68	0.08
15	445.36	—	403.31	—
16	457.02	422.47	422.80	0.08
17	457.20	428.92	428.06	−0.20
18	484.41	—	430.71	—
19	484.84	—	451.03	—
20	496.81	—	453.71	—
21	498.90	—	453.81	—
22	516.59	—	476.06	—
23	528.65	478.22	477.13	−0.23
24	551.61	—	485.94	—
25	557.68	—	490.54	—
26	560.68	—	495.24	—
27	563.08	504.72	506.36	0.33
28	565.01	508.66	511.92	0.64
29	568.89	—	521.58	—
30	569.86	—	531.23	—

Table 3: Results of engineering moduli calculations.

	Modulus	Kinney et al. [22]
E_{11}/GPa	22.641	25
E_{33}/GPa	13.637	23.2
G_{12}/GPa	10.608	8.6
G_{23}/GPa	7.742	9.4
ν_{12}	0.067	0.45
ν_{31}	0.378	0.29

In theory, the lower order resonant modes are mostly shear modes, so, in the experiment, the shear wave ultrasound transducer could get stronger signal and more accurate frequency response [30]. As shown in Figure 2, the first three orders of resonant frequencies are more obvious and the resonance peaks are sharper, but the subsequent resonance peaks become broad due to the low quality factor of dentin. When the experimental resonant frequency was extracted, the linearly predictive filtering and nonlinear least squares optimization of the experimental frequency response could make it possible for the originally gentle and overlapping resonance peaks to be distinguished.

In general, when choosing the resonant order to be calculated, the number should be at least five times the number of unknown independent elastic constants [12, 14]. For transversely isotropic solids with five independent constants, it is reasonable to choose the theoretical value of the first 30-order resonant frequency in the calculations. During the Levenberg-Marquardt iteration, the elastic tensor changes constantly, leading to the the first 30-order calculated frequency band being smaller, in which only 13 orders could match with the first 13 out of the whole 16 measured resonant frequencies. In this paper, we compared each experimental resonance frequency with the theoretical resonance frequencies and tried to figure out all the pairings. But interestingly, in most cases, the cost function will not converge to the minimum value if the pairing is incorrect. Using this method, the error of each matched pairing between experimental resonance frequency and calculated resonance frequency was all less than 0.65%, which is in accordance with the 0.8% criterion described by Migliori and Maynard [30].

Comparing the result of this study, matrix (20), with the result of Kinney et al.'s group [22], shown as matrix (9), the original elastic tensor, there are differences between each independent elastic constant. We guessed that one reason is that the experimental resonant frequency extractions after the signal processing might be more accurate, which lead to the difference compared to the extraction without signal processing method of Kinney et al.'s work. Another reason might be the individual differences among different teeth. The differences in elastic tensors also resulted in some differences in engineering moduli, mainly on E_{33} and ν_{12}.

Bernard et al. added probabilistic methods in the pairing process [13, 31], in which simulated annealing algorithm was introduced to compute the possibility of the pairing and then the calculated value could be automatically matched to the experimental value according to the probability. In our future work, we will try to introduce this algorithm into pairing process and explore the differences and advantages of present pairing methods. Moreover, we will also try to use more specimens to learn structure-function relationships and find other verification methods to RUS.

4. Conclusion

In conclusion, the elastic tensor, even Young's moduli, shear moduli, and Poisson's ratios of dentin specimen, can be accurately extracted by the signal processing method and inverse problem approach, which demonstrates that RUS is suitable for the mechanical properties measurement of low quality factor biomaterials and can provide a theoretical basis for the development of clinical dental restorative materials and the design of dental prostheses.

Conflicts of Interest

The authors have no conflicts of interest related to the manuscript.

Acknowledgments

This work was supported by the National Natural Science Foundation of China (31570945) and National Science and Technology Ministry of Science and Technology Support Program (2015BAI06B02).

References

[1] J. H. Kinney, S. J. Marshall, and G. W. Marshall, "The mechanical properties of human dentin: a critical review and re-evaluation of the dental literature," *Critical Reviews in Oral Biology & Medicine*, vol. 14, no. 1, pp. 13–29, 2003.

[2] D. Zaytsev, A. S. Ivashov, J. V. Mandra, and P. Panfilov, "On the deformation behavior of human dentin under compression and bending," *Materials Science & Engineering C Materials for Biological Applications*, vol. 41, pp. 83–90, 2014.

[3] Y.-R. Zhang, W. Du, X.-D. Zhou, and H.-Y. Yu, "Review of research on the mechanical properties of the human tooth," *International Journal of Oral Science*, vol. 6, no. 2, pp. 61–69, 2014.

[4] D. Zaytsev and P. Panfilov, "Deformation behavior of human dentin in liquid nitrogen: a diametral compression test," *Materials Science & Engineering C Materials for Biological Applications*, vol. 42, pp. 48–51, 2014.

[5] T. Lee, R. Lakes S, and A. Lal, "Investigation of bovine bone by resonant ultrasound spectroscopy and transmission ultrasound," *Biomechanics & Modeling in Mechanobiology*, vol. 1, no. 2, pp. 165–175, 2002.

[6] T. Watanabe, M. Miyazaki, H. Inage, and H. Kurokawa, "Determination of elastic modulus of the components at dentin-resin interface using the ultrasonic device," *Dental Materials Journal*, vol. 23, no. 3, pp. 361–367, 2004.

[7] M.-H. Lu, Y.-P. Zheng, and Q.-H. Huang, "A novel method to obtain modulus image of soft tissues using ultrasound water jet indentation: a phantom study," *IEEE Transactions on Biomedical Engineering*, vol. 54, no. 1, pp. 114–121, 2007.

[8] J. Du, X. L. Mao, P. F. Ye et al., "Three-dimensional reconstruction and visualization of human enamel ex vivo using high-frequency ultrasound," *Journal of Medical & Biological Engineering*, vol. 37, no. 1, pp. 112–122, 2017.

[9] D. S. Brauer, J. F. Hilton, G. W. Marshall, and S. J. Marshall, "Nano—and micromechanical properties of dentine: investigation of differences with tooth side," *Journal of Biomechanics*, vol. 44, no. 8, pp. 1626–1629, 2011.

[10] T. Inoue, M. Saito, M. Yamamoto et al., "Comparison of nanohardness between coronal and radicular intertubular dentin," *Dental Materials Journal*, vol. 28, no. 3, pp. 295–300, 2009.

[11] L. Angker, M. V. Swain, and N. Kilpatrick, "Micro-mechanical characterisation of the properties of primary tooth dentine," *Journal of Dentistry*, vol. 31, no. 4, pp. 261–267, 2003.

[12] S. Bernard, Q. Grimal, and P. Laugier, "Accurate measurement of cortical bone elasticity tensor with resonant ultrasound spectroscopy," *Journal of the Mechanical Behavior of Biomedical Materials*, vol. 18, pp. 12–19, 2013.

[13] S. Bernard, Q. Grimal, and P. Laugier, "Resonant ultrasound spectroscopy for viscoelastic characterization of anisotropic attenuative solid materials," *Journal of the Acoustical Society of America*, vol. 135, no. 5, pp. 2601–2613, 2014.

[14] A. Migliori and J. L. Sarrao, *Resonant Ultrasound Spectroscopy: Applications to Physics, Materials Measurements, and Nondestructive Evaluation*, Wiley, New York, NY, USA, 1997.

[15] A. Migliori, J. L. Sarrao, W. M. Visscher et al., "Resonant ultrasound spectroscopic techniques for measurement of the elastic moduli of solids," *Physica B: Physics of Condensed Matter*, vol. 183, no. 1-2, pp. 1–24, 1993.

[16] P. Sedlák, H. Seiner, J. Zídek, M. Janovská, and M. Landa, "Determination of all 21 independent elastic coefficients of generally anisotropic solids by resonant ultrasound spectroscopy: benchmark examples," *Experimental Mechanics*, vol. 54, no. 6, pp. 1073–1085, 2014.

[17] S. Bernard, Q. Grimal, and P. Laugier, "Development and validation of resonant ultrasound spectroscopy for the measurement of cortical bone elasticity on small cylindrical samples," *Journal of the Acoustical Society of America*, vol. 133, no. 5, pp. 3585–3593, 2013.

[18] W. M. Visscher, A. Mialiori, T. M. Bell, and R. A. Reinert, "On the normal modes of free vibration of inhomogeneous and anisotropic elastic objects," *Journal of the Acoustical Society of America*, vol. 90, no. 4, pp. 2154–2162, 1991.

[19] H. H. Demarest, "Cube-resonance method to determine the elastic constants of solids," *Journal of the Acoustical Society of America*, vol. 49, no. 3B, pp. 768–775, 1971.

[20] R. Holland, "Resonant properties of piezoelectric ceramic rectangular parallelepipeds," *Journal of the Acoustical Society of America*, vol. 43, no. 5, pp. 988–997, 1968.

[21] I. Ohno, "Free vibration of a rectangular parallelepiped crystal and its application to determination of elastic constants of orthorhombic crystals," *Journal of Physics of the Earth*, vol. 24, no. 4, pp. 355–379, 1976.

[22] J. H. Kinney, J. R. Gladden, G. W. Marshall, S. J. Marshall, J. H. So, and J. D. Maynard, "Resonant ultrasound spectroscopy measurements of the elastic constants of human dentin," *Journal of Biomechanics*, vol. 37, no. 4, pp. 437–441, 2004.

[23] A. V. Lebedev, L. A. Ostrovskiĭ, A. M. Sutin, I. A. Soustova, and P. A. Johnson, "Resonant acoustic spectroscopy at low Q factors," *Acoustical Physics*, vol. 49, no. 1, pp. 81–87, 2003.

[24] R. Kumaresan and D. W. Tufts, "Estimating the parameters of exponentially damped sinusoids and pole-zero modeling in noise," *IEEE Transactions on Acoustics, Speech, and Signal Processing*, vol. 30, no. 6, pp. 833–840, 1982.

[25] R. Kumaresan, "On the zeros of the linear prediction-error filter for deterministic signals," *IEEE Transactions on Acoustics Speech & Signal Processing*, vol. 31, no. 1, pp. 217–220, 1983.

[26] A. V. Lebedev, "Method of linear prediction in the ultrasonic spectroscopy of rock," *Acoustical Physics*, vol. 48, no. 3, pp. 339–346, 2002.

[27] L. Ostrovsky, A. Lebedev, A. Matveyev et al., "Application of three-dimensional resonant acoustic spectroscopy method to rock and building materials," *Journal of the Acoustical Society of America*, vol. 110, no. 4, pp. 1770–1777, 2001.

[28] K. Madsen, H. B. Nielsen, and O. Tinglesff, Methods for Non-Linear Least Squares Problems, Informatics and Mathematical Modelling, Technical University of Denmark, Lyngby, Denmark, 2004.

[29] A. Tarantola, *Inverse Problem Theory and Methods for Model Parameter Estimation*, SIAM: Society for Industrial and Applied Mathematics, Philadelphia, PA, USA, 2004.

[30] A. Migliori and J. D. Maynard, "Implementation of a modern resonant ultrasound spectroscopy system for the measurement of the elastic moduli of small solid specimens," *Review of Scientific Instruments*, vol. 76, no. 12, pp. 1–8, 2005.

[31] S. Bernard, G. Marrelec, P. Laugier, and Q. Grimal, "Bayesian normal modes identification and estimation of elastic coefficients in resonant ultrasound spectroscopy," *Inverse Problems*, vol. 31, no. 6, pp. 805–815, 2015.